Phase structure of strange matter

Kang Seog Lee

Department of Physics, Chonnam National University, Yong-Bong Dong, Kwangju 500, Korea

Ulrich Heinz

Institut für Theoretische Physik, Universität Regensburg, Postfach 10 10 42, W-8400 Regensburg, Germany
(Received 12 October 1992)

We present a detailed discussion of the phase structure of hadronic matter with finite strangeness content and discuss the thermodynamic conditions for the formation of metastable strange quark droplets ("strangelets") in relativistic nuclear collisions. We point out a very rich structure of the phase diagram both at zero and nonzero temperature, and study the dynamical trajectories through this diagram taken by an expanding strange fireball.

PACS number(s): 12.38.Mh, 21.65.+f, 25.75.+r

I. INTRODUCTION

The possible creation of droplets of metastable cold strange quark matter ("strangelets") in relativistic nuclear collisions, which was suggested by Liu and Shaw [1] and Greiner *et al.* [2] following ideas by Witten [3] and Farhi and Jaffe [4], has recently attracted a lot of theoretical [5, 6] and experimental [7] interest due to its potential of serving as a unique and unmistakable signature for quark-gluon plasma formation in the laboratory. While in the early Universe the slow expansion allows equilibrium to be maintained with respect to the weak interactions, which convert strange into nonstrange quarks and vice versa in such a way that the free energy is always minimized, the situation in heavy-ion collisions is quite different: the short collision time scales suppress weak processes, and strangeness has to be considered as a conserved quantum number. This difference is crucial: in the early Universe adiabatic β equilibration leads to the "boiling off" of any strange quark matter lumps possibly created in the hadronization phase transition [8]; in heavy-ion collisions, strangeness conservation, together with the mechanism of "s-$\bar{s}$ separation" during the phase transition [9, 10, 2] and via surface emission of hadrons [5, 6], opens the possibility that metastable strange quark matter droplets could survive the expansion and cooling stages of the hot collision fireball [2, 6].

To properly plan strangelet search experiments, realistic estimates of their formation rates would be highly desirable. Unfortunately, existing calculations [2, 6] of the dynamical evolution of the hot collision zone and of its strangeness content are still rather schematic and do not even allow to reliably predict the correct order of magnitude. One of the reasons is the strong sensitivity of the relative stability of the strangelets and of their decay rates on model parameters such as the bag constant [2, 6]. On the other hand, too little is still known about the phase structure of strange matter and the thermodynamic path followed by the fireball through the phase diagram during the expansion and cooling stage.

In this paper we present a comprehensive and careful study of the phase structure of cold and hot strange matter, which uncovers a rich structure in the strange sector of the phase diagram and thus supplements the partial knowledge on this subject documented in [2–6]. While in this work we do not yet attempt to also improve on the calculations for the dynamical evolution of the collision zone, we believe that the work presented here can serve as a complete and reliable thermodynamic basis for such calculations in the future. The way in which we present the results leads to an intuitive understanding of the conditions which have to be met in order to dynamically create cold strange quark matter. They helped us (and hopefully will do the same for the reader) to understand the results obtained in [2, 6], and they should provide useful consistency checks on future dynamical calculations.

We begin our discussion in Sec. II with a short summary of the equation of state which we employ. Sec. III is dedicated to a detailed discussion of the phase structure at zero temperature. It exhibits some very interesting and unexpected structures which to our knowledge have so far escaped notice. In Sec. IV we extend the phase diagram to nonzero temperature and show, in the three-dimensional space spanned by the temperature and the two chemical potentials associated with baryon number and strangeness, the regions of phase coexistence for systems with varying degrees of strangeness. In Sec. V we discuss the expansion trajectories of hot and dense strange systems through the phase diagram. We will analyze under which conditions the system will "get stuck" in the phase coexistence region, thus never hadronizing completely and giving rise to surviving (meta)stable cold quark matter droplets. Section VI finally summarizes our main results, while the Appendix provides the reader with some useful expressions for the evaluation of the relevant thermodynamic quantities.

II. THE EQUATION OF STATE

A. The quark-gluon plasma phase

The quark-gluon plasma (QGP) phase is assumed to consist of free quarks and gluons. We will always set $\alpha_s = 0$ in the QGP phase; it has been shown in [11] that

the effects of $\alpha_s \neq 0$ can to a large degree be absorbed by a reparametrization of the bag constant B. We thus take B as a phenomenological parameter which can vary freely. We consider three quark species, i.e., massless up and down quarks and massive ($m_s \simeq 150$ MeV) strange quarks.

All the thermodynamic variables can be easily obtained from the thermodynamic potential Ω. The pressure $P = -\Omega/V$ can be written in terms of temperature and chemical potentials as

$$P_Q = -B + \frac{37}{90}\pi^2 T^4 + \mu_q^2 T^2 + \frac{1}{2\pi^2}\mu_q^4$$
$$+ \frac{1}{\pi^2}\int_{m_s}^{\infty} dE(E^2 - m_s^2)^{3/2}\left(\frac{1}{e^{\beta(E-\mu_q+\tilde{\mu}_s)}+1} + \frac{1}{e^{\beta(E+\mu_q-\tilde{\mu}_s)}+1}\right). \tag{1}$$

Here B is the MIT bag constant which is needed to simulate the background confinement pressure; μ_q is the light quark chemical potential and equals one third of the baryon chemical potential, $\mu_q = \mu_b/3$; and $\tilde{\mu}_s$ is the chemical potential associated with the quantum number strangeness. Since a strange quark carries both baryon number $1/3$ and strangeness -1, the chemical potential for the strange quark, μ_s, can be written as $\mu_s = \mu_q - \tilde{\mu}_s$.

The baryon number density is given by

$$\rho_b = \frac{1}{3}\left(\frac{\partial P}{\partial \mu_q}\right)_T = \frac{1}{3}(\rho_q + \rho_s), \tag{2}$$

where ρ_q is the net light quark density while ρ_s is the net strange quark density (i.e., minus the strangeness density) and given by

$$\rho_s = \left(\frac{\partial P}{\partial \mu_s}\right)_T = -\left(\frac{\partial P}{\partial \tilde{\mu}_s}\right)_T, \tag{3}$$

or explicitly

$$\rho_s = \frac{6}{2\pi^2}\int_{m_s}^{\infty} dE\, E\, (E^2 - m_s^2)^{1/2}$$
$$\times \left(\frac{1}{e^{\beta(E-\mu_s)}+1} - \frac{1}{e^{\beta(E+\mu_s)}+1}\right). \tag{4}$$

B. Hadronic matter

We consider hadronic matter as a weakly interacting gas of pions, nucleons, and baryonic and mesonic resonances. We add hard core repulsion, which is essential for the existence of a phase transition in our model, via a proper volume correction. The expression for the pressure is

$$P_H = \frac{1}{1 + \varepsilon^{\mathrm{pt}}/4B}\sum_i P_i^{\mathrm{pt}}, \tag{5}$$

where

$$P_i^{\mathrm{pt}} = \frac{d_i}{6\pi^2}\int_{m_i}^{\infty} dE\,\frac{(E^2 - m_i^2)^{3/2}}{e^{\beta(E-\mu_i)}\pm 1}. \tag{6}$$

Here d_i is the degeneracy factor, and the superscript "pt" denotes the thermodynamic expressions for pointlike particles. The chemical potential of each particle i is written

as a combination of μ_q and μ_s:

$$\mu_i = (n_i^q - n_i^{\bar{q}})\mu_q + (n_i^s - n_i^{\bar{s}})\mu_s, \tag{7}$$

where $(n_i^q - n_i^{\bar{q}})$ is the net number of light valence quarks and $(n_i^s - n_i^{\bar{s}})$ is the net number of strange valence quarks contained in hadron species i.

The factor $(1 + \varepsilon^{\mathrm{pt}}/4B)^{-1}$ is the proper volume correction [12] and limits the energy density to $4B$, i.e., the value inside a hadron according to the MIT bag model.

Using the relations (2) and (3), we can derive equations for the baryon and strangeness density. Through the above relation between the chemical potentials, the baryon density is related to the particle densities ρ_i^{pt} by

$$\rho_b^{\mathrm{pt}} = \sum_i b_i \rho_i^{\mathrm{pt}}, \tag{8}$$

where b_i is the baryon number of ith particle species. Similarly, the net strange valence quark density (i.e., minus the strangeness density) is given by

$$\rho_s^{\mathrm{pt}} = -\sum_i s_i \rho_i^{\mathrm{pt}}, \tag{9}$$

where s_i is the strangeness of the ith particle species. For later use, ρ_i^{pt} is written down explicitly as

$$\rho_i^{\mathrm{pt}} = \frac{d_i}{2\pi^2}\frac{m_i^2}{\beta}\sum_{n=1}^{\infty}\frac{(\mp)^{n+1}}{n}K_2(n\beta m_i)e^{n\beta\mu_i}. \tag{10}$$

The physical densities are obtained from the point particle densities through a proper volume correction:

$$\rho_i = \frac{1}{1 + \varepsilon^{\mathrm{pt}}/4B}\,\rho_i^{\mathrm{pt}}. \tag{11}$$

III. THE PHASE DIAGRAM AT ZERO TEMPERATURE

The system we consider has finite strangeness and undergoes (by construction) a first order phase transition from a QGP phase to the hadronic phase. The equilibrium phase diagram can be obtained from the two-phase equilibrium conditions $P_H = P_Q$, $T_H = T_Q$, $\mu_{q,H} = \mu_{q,Q}$, and $\mu_{s,H} = \mu_{s,Q}$. By setting the temperatures and chemical potentials in the two phases equal, this leads to the

usual pressure balance relation between the two phases:

$$P_H(T, \mu_q, \mu_s) = P_Q(T, \mu_q, \mu_s). \tag{12}$$

We parametrize the finite strangeness through the strangeness fraction

$$f_s = \frac{\rho_s(T, \mu_q, \mu_s)}{\rho_b(T, \mu_q, \mu_s)}, \tag{13}$$

i.e., the net number of strange (valence) quarks per baryon (or minus the strangeness per baryon).

For various values of the strangeness fraction f_s, we can determine the phase diagram by solving Eq. (12) at fixed T for μ_q and μ_s under the constraint Eq. (13).

As pointed out in Refs. [9,10], the phase diagram with strangeness needs a little caution. The phase transition takes place through the mixed phase, which is a mixture of the two phases, and is parametrized by the volume fraction $\alpha = V_H/(V_H + V_Q)$ as the system converts continuously from QGP phase to hadronic phase. For example, $\alpha = 0$ when the hadronization starts, and $\alpha = 1$ at the end of the hadronization. The equilibrium conditions should be applied at any point in the mixed phase with the constraint that the system as a whole maintains the given strangeness fraction f_s. (It is not appropriate to constrain a certain value of f_s separately in each phase.) This procedure causes a smooth variation of the chemical potentials μ_q and μ_s during the conversion from QGP to hadronic matter.

Using the equations of state in Sec. II, the phase diagram is obtained numerically from Eqs. (12) and (13). However, in the limit $T \to 0$ the solution of these equations is a little tricky, and a careful analysis reveals many interesting facts as to which particles dominate the hadronic phase at small T for various values of the strangeness fraction f_s. This will be discussed in Sec. III C.

A. The line of phase coexistence in the limit $T \to 0$

We will consider only systems with positive baryon number and positive values of f_s (i.e., more strange quarks than antiquarks, resulting in negative strangeness). With the help of Eq. (2) the condition $f_s = \rho_s/\rho_b$ can be rewritten as

$$\rho_s = \frac{f_s}{3 - f_s} \rho_q. \tag{14}$$

From this one sees that for $f_s \geq 3$, $\rho_q \leq 0$. If the system is in the quark phase, $f_s > 3$ thus implies that the light quark chemical potential μ_q^Q becomes negative, and at the beginning of hadronization nonstrange antibaryons would then be more abundant than nonstrange baryons. For $f_s = 3$, Eq. (13) is solved in the quark phase by $\mu_q^Q = 0$, and the first hadronic bubbles appearing during hadronization will contain equal numbers of non-strange baryons and antibaryons. Since such an extreme situation appears hard to realize in nature, we will limit ourselves to the region $0 \leq f_s \leq 3$.
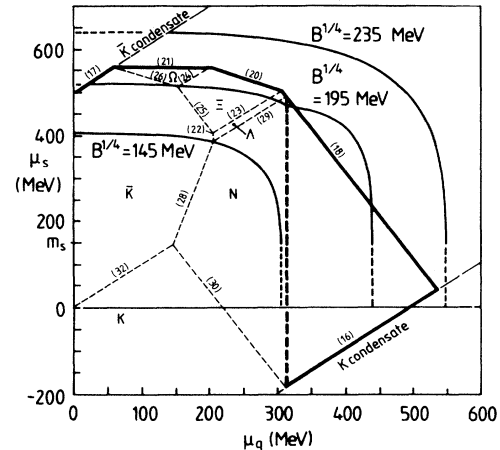
The solution of the pressure equilibrium equation (12)

FIG. 1. Phase structure at $T = 0$. The three solid curves are the phase coexistence lines for $B^{1/4} = 145, 195, 235$ MeV, respectively. Inside the region defined by the thick solid and dashed lines no hadrons exist at $T = 0$. This region is divided into 6 small regions, where (as indicated) certain particle species dominantly contribute to f_s at low temperatures.

yields a critical line $\mu_s(\mu_q)$ in the $T = 0$ plane which separates the QGP from the hadronic phase. It is easily evaluated using the analytic form Eq. (A11) of the $T = 0$ pressure integrals. Since at $T = 0$ only fermions contribute to the pressure, and only do so if their chemical potentials satisfy $\mu_i > m_i$, only very few particles play a role on the hadronic side. In fact, if the light quark chemical potential drops below $\mu_q = m_N/3$ before μ_s has reached the limit for a nonvanishing Fermi sea of hyperons, $\mu_s \geq m_\Lambda - 2\mu_q$, the hadronic pressure collapses to zero at this point, and in the region $\mu_q \leq m_N/3$ the pressure balance equation degenerates to the equation $P_Q = P_H = 0$.

The resulting phase coexistence line at $T = 0$, for f_s in the range $0 \leq f_s \leq 3$, is shown in Fig. 1 for three values of the bag constant, $B^{1/4} = 145, 195$, and 235 MeV, respectively, which roughly span the range usually considered as realistic.[1] The phase coexistence line at $T = 0$ for a specific value of f_s corresponds to a certain section of these lines, as will be discussed in detail later.

The phase coexistence line shows characteristic kinks and discontinuities which require a careful discussion.

For $B^{1/4} = 145$ MeV, the phase coexistence line lies entirely in the region $\mu_q < m_N/3$ where at $T = 0$ no baryons survive. Thus the pressure in the hadronic phase is zero, and the phase coexistence line is identical with the curve $P_Q = 0$. Note that for $P_Q = 0$ the quark matter is in mechanical equilibrium with the outside vacuum pressure (B) and cannot expand; i.e., *the QGP phase is mechanically stable*. Since in this case this condition is satisfied everywhere on the phase coexistence curve (i.e.,

---

[1]The other lines shown in Fig. 1 will be explained in Sec. III C.

for all values of f_s), weak interactions which change f_s have no influence on the stability of the quark matter, i.e., in this case cold (strange and nonstrange) quark matter is *absolutely stable*.

For $B^{1/4} = 195$ MeV, there occurs a kink at $\mu_q = m_N/3$, i.e., at the point where the pressure in the hadron gas becomes zero. All points on the critical line to the left of this value have again $P = 0$, i.e., correspond to mechanically stable quark matter with finite net strangeness f_s (see Secs. III B and III C). In this case weak interactions could, in principle, move the system along the phase coexistence region towards the right by reducing f_s until it reaches $f_s = 0$ and begins to hadronize into a nonstrange hadron gas. Thus in this case strangelets would in general only be metastable (i.e., stable with respect to strong interactions, but not with respect to weak interactions). In the region $\mu_q > m_N/3$ the pressure along the critical line is a continuously rising function of μ_q until μ_s drops below the strange quark mass m_s. At this point the phase diagram shows for all values of B another discontinuity, which will be discussed in the following subsection.

Please note that a given pair of numbers (μ_q, μ_s) corresponds to different values of f_s in the Q and H phases, respectively, since the densities ρ_q, ρ_s behave discontinuously in a first order phase transition. Hence, as α changes from 0 to 1 during the hadronization, f_s changes continuously if (μ_q, μ_s) are held fixed. In other words, for hadronization at constant f_s, the variables (μ_q, μ_s) evolve continuously, generating a trajectory in the phase diagram. In the mixed phase these trajectories follow for a while the phase coexistence line. This is seen in Figs. 2 and 3, where lines of constant strangeness fraction f_s at $T = 0$ are shown for $B^{1/4}= 195$ and 235 MeV, respectively. Details of the (f_s=const) lines in each phase will be discussed later.
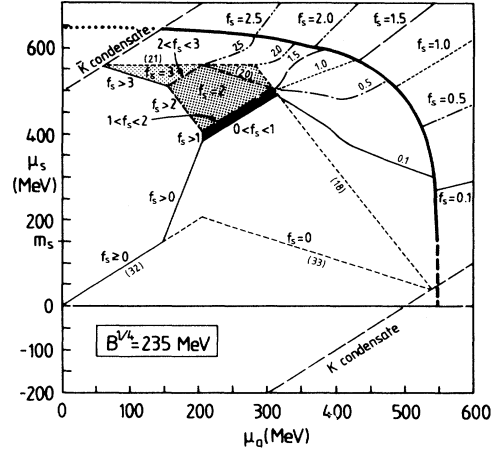
FIG. 3. Same as Fig. 2, but for $B^{1/4} = 235$ MeV. For this bag constant the phase coexistence line stays outside of the thick solid line in Fig. 1, and quark matter droplets with arbitrary strangeness content hadronize completely by expansion.

B. The boundary between QGP and mixed phase in the limit $T \to 0$

At the boundary between QGP and mixed phase ("QM phase boundary"), i.e., for $\alpha = 0$, all matter is still in the quark phase, and thus f_s has to be evaluated using the QGP expressions for the densities $f_s = \rho_{s,Q}/\rho_{b,Q}$. We will suppress the index Q in the following, but it will always be implied in this subsection.

At $T = 0$ and for $\mu_i > m_i$, all the thermal integrations can be done analytically (see Appendix A 3). For nonzero values of f_s, we obtain in this limit from $\rho_q = (2/\pi^2)\mu_q^3$ and Eq. (14) the identity

$$\mu_s^2 = m_s^2 + a\,\mu_q^2, \tag{15}$$

where $a = [2f_s/(3 - f_s)]^{2/3}$. From this relation, it is easy to check that for $f_s \geq 1$ ($a \geq 1$), μ_s is always larger than μ_q. For $f_s < 1$ ($a < 1$), $\mu_s < \mu_q$ when $\mu_s > m_s/\sqrt{1 - a}$, and $\mu_s > \mu_q$ when $\mu_s < m_s/\sqrt{1 - a}$. This was used to check the numerical results.

It is interesting to observe the discontinuous behavior of μ_s as a function of the strangeness fraction f_s: In order to have nonzero strangeness in the quark phase ($f_s > 0$), μ_s has to exceed m_s for small values of T. On the other hand, for systems with zero strangeness ($f_s = 0$) μ_s vanishes identically at all temperatures $T \neq 0$ along the QM phase boundary, in order to balance strangeness from strange quarks and antiquarks. Hence it seems natural to analytically continue this value $\mu_s = 0$ for $f_s = 0$ also to $T = 0$. Since, however, for $\mu_s < m_s$, no strange quarks remain in the QGP phase as $T \to 0$, $\mu_s(T = 0)$ has then to jump from 0 to values larger than m_s as soon as the system acquires nonzero net strangeness $f_s > 0$. Similarly, $\mu_s(T = 0)$ jumps to values below $-m_s$ when f_s turns negative. Altogether, $\mu_s(T = 0)$ jumps by $2m_s$ (namely from $\mu_s = -m_s$ to $\mu_s = +m_s$) as f_s passes in the quark phase through zero from negative to positive values. As seen in Fig. 1, for $B^{1/4} = 195$ MeV this jump
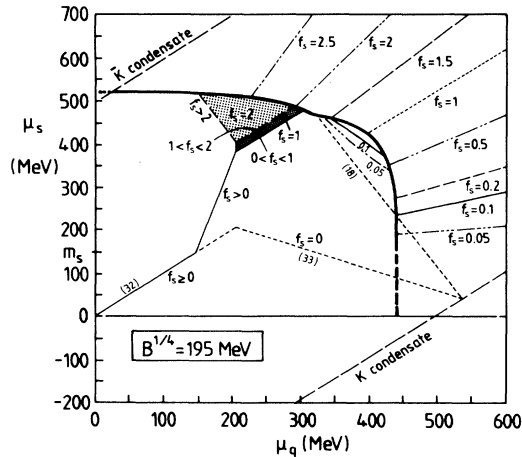

FIG. 2. Lines of constant strangeness fraction f_s for $B^{1/4} = 195$ MeV. All trajectories with $f_s > 0$ eventually end up in a mixed phase at zero pressure, corresponding to mechanically stable cold strange quark matter droplets. For a detailed discussion see text.

occurs at $\mu_q \simeq 441$ MeV.

The crossing points of f_s=const lines from the QGP phase with the critical line in Figs. 2, 3 show that, as f_s increases along the QM phase boundary, μ_q decreases and μ_s increases smoothly until the limit $\mu_q = 0$ is reached at $f_s = 3$. This smooth variation of f_s along the QM boundary is seen explicitly in Fig. 4. [However, contrary to the QM boundary, f_s at the hadron and mixed phase boundary shows discontinuities, as will be discussed below in Sec. III D.]

Equation (15) holds also in the pure QGP phase and can be used to understand the numerical results for lines of constant f_s in the QGP phase shown in Figs. 2 and 3. The lines look nearly straight because $a\mu_q^2$ is much smaller than m_s^2 in Eq. (15). Since Eq. (15) is independent of the bag constant B, the lines in Figs. 2 and 3 corresponding to the same values of f_s are identical in the QGP phase.

C. Particle composition of the hadron gas near $T = 0$ in the different regions of the μ_q-μ_s plane

In order to better understand the behavior of f_s on the hadronic side of the phase transition, it is necessary to analyze the composition of the hadron gas at low temperatures before we discuss the hadronic and mixed phase (HM) boundary in the following subsection.

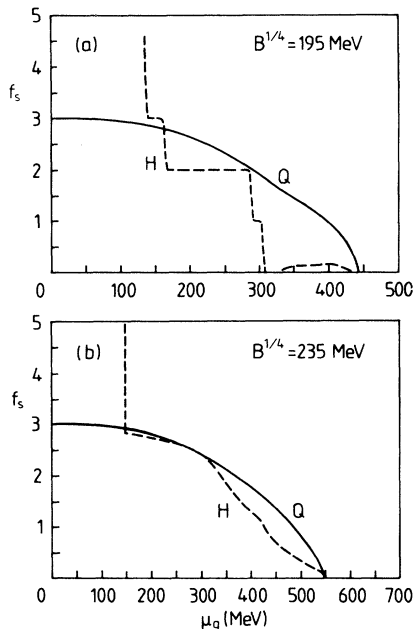(1) For kaons, which are bosons, Bose-Einstein con-

FIG. 4. Values of f_s at the QM and HM boundaries along the phase coexistence line for (a) $B^{1/4} = 195$ MeV and (b) $B^{1/4} = 235$ MeV. Please note in case (a) the discontinuous behavior of f_s as a function of μ_q in the hadronic phase, which accompanies the possibility of strangelet formation. The singularity of f_s at small values of μ_q is caused by kaon condensation.

densation occurs when $\mu_K = m_K$. Allowed regions for the chemical potentials are

$$\mu_s \geq \mu_q - m_K \quad (m_K = m_{\bar{K}} = 496 \text{ MeV}), \quad (16)$$

$$\mu_s \leq \mu_q + m_{\bar{K}} . \quad (17)$$

At the borders of these regions, there will be finite densities for K or $\bar{K}$, respectively, in the limit $T = 0$. Our idealized hadronic equation of state of pointlike particles does not exist outside of these borders; an extension beyond these limits would require the introduction of particle-specific repulsive forces between the kaons [13] rather than the across-the-board proper volume correction employed by us.

(2) For strange baryons, there are finite number densities at $T = 0$ when $\mu_i \geq m_i$:

$$\Lambda : \quad \mu_s \geq -2\mu_q + m_\Lambda \quad (m_\Lambda = 1116 \text{ MeV}), \quad (18)$$

$$\Sigma : \quad \mu_s \geq -2\mu_q + m_\Sigma \quad (m_\Sigma = 1189 \text{ MeV}), \quad (19)$$

$$\Xi : \quad \mu_s \geq (-\mu_q + m_\Xi)/2 \quad (m_\Xi = 1315 \text{ MeV}), \quad (20)$$

$$\Omega : \quad \mu_s \geq m_\Omega/3 \quad (m_\Omega = 1672 \text{ MeV}). \quad (21)$$

In Fig. 1 we show these limits which separate regions of finite and vanishing densities for the various strange particle species in the limit $T = 0$: The thick solid line is a combination of Eqs. (16)–(21); it separates those regions, in which no strange particles survive at all in the limit $T \to 0$, from those where at least one strange particle species has finite density at $T = 0$.[2] A cold hadron gas with $f_s > 0$ and nonzero density can only exist to the right of the thick solid line.

This has important consequences: If throughout the region to the upper right of the solid line the pressure in the quark phase happens to be larger than in the hadronic phase (this is the case for $B^{1/4} < 180$ MeV, see Fig. 1), strange quark matter with $f_s > 0$ will be the stable ground state at $T = 0$. A hypothetical cold strange quark matter droplet created somewhere in the upper right of Fig. 1 will expand due to its Pauli pressure, following one of the f_s=const trajectories of Figs. 2 and 3 until it reaches the phase coexistence line. At that point it will begin to hadronize, thereby moving along the coexistence line to the left until it reaches the kink, i.e., the point at which the pressure vanishes. At this point the expansion and hadronization process stops, and whatever fraction α of quark matter is still left will stay there forever. Thus, if the phase coexistence line at $T = 0$ passes through the region left of the thick solid line, strangelet formation is (in principle) possible. If this is not the case (i.e., if B is sufficiently large, $B \gtrsim 208$ MeV in our case), strange quark matter will always hadronize completely [2].

The thick dashed line in Fig. 1 includes also non-strange particles: since for $\mu_q < m_N/3$ no nucleons can exist at $T = 0$, the region left of the thick dashed line is

---

[2]Equation (19) is not shown since its validity automatically implies Eq. (18), which is thus the stronger condition.

completely empty of particles at $T = 0$, and a cold hadron gas of any type ($f_s = 0$ or $f_s \neq 0$) can only exist with non-zero density in the region right of this line. Thus, if B is chosen so small that the phase coexistence line is entirely in the region $\mu_q < m_N/3$ (as seen in Fig. 1, with our equation of state this is true for $B \lesssim 148$ MeV), then even non-strange quark matter will be stable at $T = 0$.

To the left of the thick dashed line particles only exist at nonzero temperature. To understand the behavior of f_s (which is in this region given by a ratio of densities which both vanish in the limit $T \to 0$), we will now discuss which particles dominate as T approaches 0. This is done using the low-temperature expansion of the Bose and Fermi distributions in the region $\mu_i < m_i$ as given in Appendix A 2. Since in this limit only the leading Boltzmann term ($n = 1$) of the expansion contributes, it is quite easy to find out for each pair (μ_q, μ_s) which particle species has the largest density: all densities go $\sim \exp[-\beta(m_i - \mu_i)]$, and one only needs to compare the magnitude of ($m_i - \mu_i$).

(1) $\bar{K}$ dominates over Λ as long as $\mu_s - \mu_q - m_K \geq 2\mu_q + \mu_s - m_\Lambda$:

$$\mu_q \leq \frac{1}{3}(m_\Lambda - m_K) = 207 \text{ MeV}. \tag{22}$$

(2) Λ dominates over Ξ as long as $2\mu_q + \mu_s - m_\Lambda \geq \mu_q + 2\mu_s - m_\Xi$:

$$\mu_s \leq \mu_q + 199 \text{ MeV}. \tag{23}$$

(3) Ξ dominates over Ω as long as $\mu_q + 2\mu_s - m_\Xi \geq 3\mu_s - m_\Omega$:

$$\mu_s \leq \mu_q + 357 \text{ MeV}. \tag{24}$$

(4) $\bar{K}$ dominates over Ξ as long as $\mu_s - \mu_q - m_K \geq \mu_q + 2\mu_s - m_\Xi$:

$$\mu_s \leq -2\mu_q + 819 \text{ MeV}. \tag{25}$$

(5) $\bar{K}$ dominates over Ω as long as $\mu_s - \mu_q - m_K \geq 3\mu_s - m_\Omega$:

$$\mu_s \leq -\frac{1}{2}\mu_q + 588 \text{ MeV}. \tag{26}$$

(6) $\bar{K}$ dominates over K as long as $\mu_s - \mu_q - m_K \geq \mu_q - \mu_s - m_K$:

$$\mu_s \geq \mu_q . \tag{27}$$

Finally, it will also be interesting to compare with nucleons.

(7) Nucleons dominate over $\bar{K}$ as long as $3\mu_q - m_N \geq \mu_s - \mu_q - m_K$:

$$\mu_s \leq 4\mu_q - 443 \text{ MeV}. \tag{28}$$

(8) Nucleons dominate over Λ as long as $3\mu_q - m_N \geq \mu_s + 2\mu_q - m_\Lambda$:

$$\mu_s \leq \mu_q + 177 \text{ MeV}. \tag{29}$$

In this region Λ dominates over Ξ and Ω, so nucleons are also more abundant than these multistrange baryons.

(9) Nucleons dominate over K as long as $3\mu_q - m_N \geq \mu_q - \mu_s - m_K$:

$$\mu_s \geq -2\mu_q + 443 \text{ MeV}. \tag{30}$$

These results are drawn in Fig. 1 in thin short-dashed lines. They divide the region below the thick lines into 6 smaller regions, where (as indicated) certain particle species dominantly contribute to f_s.

As strange particles we consider $\bar{K}$ ($= \bar{K}^0 + K^-$), Λ, Σ, Ξ, Ω in the sector of negative strangeness, and K ($= K^0 + K^+$) in the positive strangeness sector. Compared to baryons, all antibaryons can be safely neglected in ρ_s or ρ_b near $T = 0$, as long as $f_s \leq 3$. Then

$$\rho_s = \rho_{\bar{K}} + \rho_\Lambda + \rho_\Sigma + 2\rho_\Xi + 3\rho_\Omega - \rho_K . \tag{31}$$

Since in the limit $T \to 0$ for each point (μ_q, μ_s) the hadronic phase is dominated by one single particle species, it is (at least in the region to the left of the thick solid line in Fig. 1) quite easy to figure out which value f_s is assumed:

Since nucleons possess no strangeness, the N-dominated region corresponds to $f_s = 0$. Similarly, the Λ-, Ξ-, and Ω-dominated regions correpond to $f_s = 1, 2$, and 3, respectively. The $\bar{K}$- and K-dominated regions correspond to $f_s = +\infty$ and $-\infty$, respectively. Any other values of f_s have to correspond to lines separating these regions in Fig. 1. For example, systems with $f_s = 2.5$ have to be either on the line separating Ξ from Ω or the one separating Ξ from $\bar{K}$. A system with $f_s = 3$ is either in the Ω-dominated region, or on the line separating Ξ from $\bar{K}$ (with equal Ξ and $\bar{K}$ densities), or on the line separating Λ from $\bar{K}$ (with twice as many $\bar{K}$ as Λ).

The resulting lines of constant f_s in the hadronic phase at zero temperature are shown in Figs. 2 and 3. We see that, as a function of μ_q and μ_s, f_s behaves quite discontinuously in the hadronic phase at $T = 0$.

D. The boundary between hadronic and mixed phase in the limit $T \to 0$

The analysis of the previous subsection can now be applied to the boundary between hadronic and mixed phase ("HM phase boundary"), where $\alpha = 1$ and f_s has to be evaluated with the hadron gas expressions for all particle densities.

In Fig. 4, values for f_s are shown as a function of μ_q along the HM and QM phase boundaries. The discontinuous behavior of f_s in the hadronic phase reflects itself in the steplike function labeled H in Fig. 4(a) for $B^{1/4} = 195$ MeV. In contrast to this, f_s behaves quite continuously in the quark phase.

For $B^{1/4} \lesssim 180$ MeV, the phase coexistence line never crosses the thick solid line in Fig. 1 into the region with finite Λ density. Systems with $f_s > 0$, moving during hadronization along the phase coexistence line towards the upper left, thus automatically end up in the region left to the thick dashed line of Fig. 1 where the pressure is zero. They thus end in a mixed phase state with mechanically stable quark matter droplets.

For $B^{1/4} = 195$ MeV, the phase coexistence line spends

a short interval in the region with finite Λ density, but f_s never exceeds a value of about 0.174 there. In this case, an expanding cold quark system with $0 < f_s < 0.174$ suffers a very strange fate: while it expands under its Pauli pressure and begins to hadronize, it first moves along the phase boundary until it reaches the region just mentioned, at which point hadronization is complete. As shown in Fig. 2 for the specific cases $f_s = 0.05$ and 0.1, further expansion occurs inside the hadronic phase along an f_s=const contour. However, the system soon reaches again the phase coexistence line, i.e., quark matter bubbles again begin to grow inside the hadronic phase. The system then expands along the phase coexistence line until it reaches at $\mu_q = m_N/3$ the region of zero baryon density where the hadronic pressure is zero, thus ending up in a state where part of the matter remains in the form of mechanically stable strange quark droplets (strangelets). For this value of B, cold systems with $f_s > 0$ thus never possess a stable pure hadron phase; such a state will expand, and some part of the material will spontaneously convert back into quark matter.

In order for cold systems with finite strangeness to be able to hadronize completely, the phase coexistence line should stay outside the thick solid line in Fig. 1. As mentioned above, the minimum value of the bag constant, for which this occurs with our equation of state, is $B^{1/4} \simeq 208$ MeV.

In Fig. 4(b) we show the behavior of f_s along the phase coexistence line for $B^{1/4} = 235$ MeV, i.e., a bag constant above this critical value. Now the behavior of f_s is continuous both in the quark matter and hadronic phase, because the particle composition in the hadronic phase at $T = 0$ changes continuously in the region outside the thick solid line of Fig. 1.

As seen in Fig. 1, for $B^{1/4} \gtrsim 180$ MeV the phase coexistence line reaches at low values of μ_q the threshold for $\bar{K}$ condensation in the hadronic phase. At this point f_s goes to infinity, as can be seen in Fig. 4. Since for the ideal hadron gas which we employ (and which does not specifically include repulsive interactions between kaons [13]) the region left of the line $\mu_s - \mu_q = m_K$ is forbidden, this implies that for sufficiently large values of B and strangeness fractions near $f_s = 3$ the chemical potentials behave in a discontinuous way during hadronization, jumping from near the μ_s axis directly to the antikaon condensation line. An analogous phenomenon with kaons, which occurs in strangeness neutral systems at low temperatures near the μ_q axis, if B is sufficiently large, was observed in [10]. Thus, if conditions are such that the strangeness of the system can in the hadron phase only be absorbed by an (anti)kaon condensate, the Gibbs condition requiring continuity of the chemical potentials cannot be satisfied. Fortunately, it appears very unlikely that such conditions can be reached in a heavy ion collision, and therefore we will not deal with this problem any further.

E. Strangeness neutrality near $T = 0$

To complete this section, we will discuss the HM phase boundary near $T = 0$ for strangeness-neutral systems ($f_s = 0$). This is necessary because there is a discontinuity of μ_s in the hadronic phase as strangeness is added to a strangeness-neutral system, in a similar way as for the quark phase (see Sec. III B). For $B^{1/4} = 195$ MeV, at the HM phase boundary (μ_q, μ_s) lies in the region dominated by Λ's and nucleons, and the negative strangeness from the Λ's can only be balanced by kaons. The exact location of the critical μ_q-μ_s line at $T = 0$ depends on the choice of B, and larger values of B will shift it to larger values of μ_q and/or μ_s. As μ_q increases we go in the hadronic phase from the $K - \bar{K}$ dominated region through the $K - \Lambda$ dominated region, eventually reaching the region with finite hyperon density at $T = 0$. In this latter region strangeness neutrality at $T = 0$ can only be ensured by the presence of a K condensate.

As discussed in [10], the line of zero strangeness in the hadronic phase is given by

$$\mu_s = \mu_q \tag{32}$$

for $\mu_q < (m_\Lambda - m_K)/3$, i.e., in the region where the system is dominated by kaons and antikaons, and by

$$\mu_s = -\frac{1}{2}\mu_q + 310 \text{ MeV} \tag{33}$$

for $(m_\Lambda - m_K)/3 < \mu_q < (m_\Lambda + m_K)/3$. Finally, for $\mu_q > (m_\Lambda + m_K)/3$, the kaon condensation threshold is reached [μ_s is large enough to support a finite density of Λ's at $T = 0$, whose strangeness can only be balanced by a kaon condensate, see Eq. (16)]:

$$\mu_s = \mu_q - m_K .$$

The heavier multistrange baryons play no role in the strangeness balance for zero-temperature $f_s = 0$ systems since they are always dominated by hyperons.

The combinations of these three conditions for $f_s = 0$ are also shown in Figs. 2 and 3.

IV. THE PHASE STRUCTURE AT FINITE TEMPERATURE

To obtain the phase diagram at finite temperature, Eq. (12) together with the constraint Eq. (13) have to be solved numerically. In the (T, μ_q, μ_s) space, the phase coexistence region describes in general an igloolike surface. By fixing the strangeness fraction f_s one cuts a strip from this surface; this is shown in Figs. 5(a)–5(f) for $B^{1/4} = 180$ MeV and various values of f_s. The strip corresponding to the phase coexistence region is projected on each of the three coordinate planes. The intersections of the whole igloo with the coordinate planes are also shown as dashed lines for orientation.

If a system with $f_s = 0$ hadronizes at fixed temperature, μ_q stays nearly constant while μ_s increases rapidly, cutting a nearly vertical strip from the lower part of the igloo wall [10]. As f_s begins to take on positive values, μ_q also begins to change appreciably during hadronization, usually decreasing from larger initial values in the quark phase to lower final values in the hadronic phase. As one approaches the extreme value $f_s = 3$, however, this tendency reverses: in the quark phase the net quark
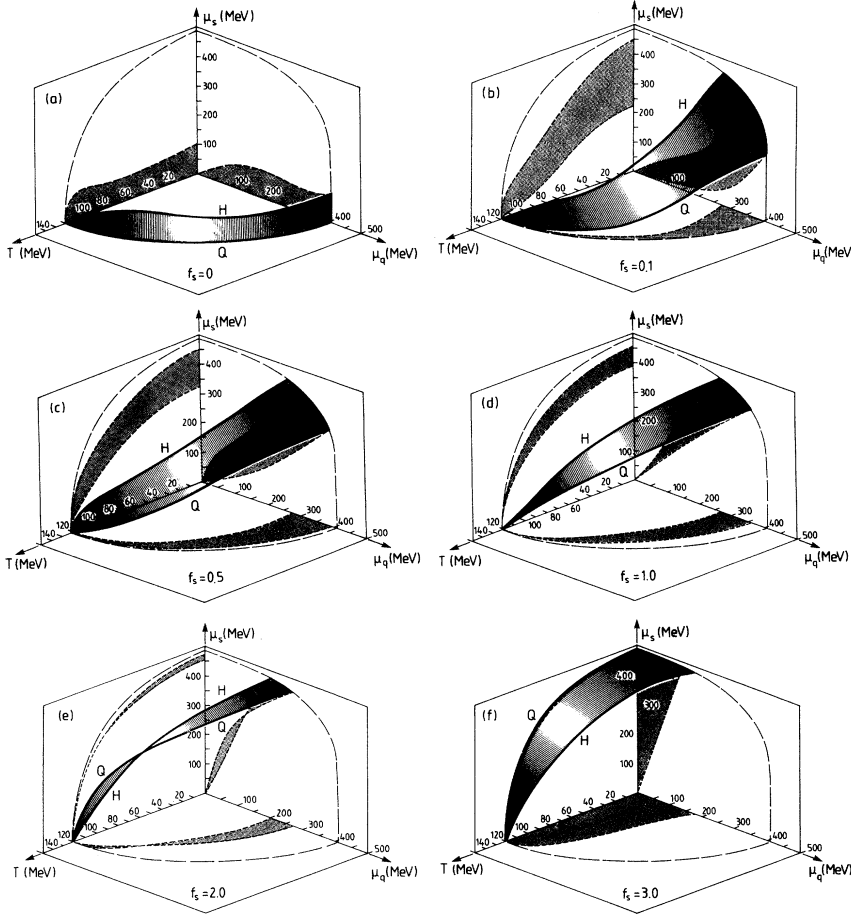
FIG. 5. The phase diagram of strongly interacting matter in (T, μ_q, μ_s) space for $B^{1/4} = 180$ MeV. The igloo-type surface describes the phase coexistence region (mixed phase) between quark matter (outside) and hadronic matter (inside). Figures (a) through (f) show various sections through this surface corresponding to systems with fixed strangeness fraction f_s. Also shown are the projections of the mixed phase region onto the three coordinate planes.

excess (i.e., the net baryon number) is purely strange, and at the onset of hadronization the baryon chemical potential μ_q is zero, building up to positive values during hadronization [see Fig. 5(f)]. For intermediate values of f_s (> 2), we observe a turning over of the magnitude of μ_q during hadronization: in Fig. 5(e), μ_q is larger at the quark boundary than at the hadron boundary, if the temperature is small, while at high temperatures the situation is exactly opposite.

V. ISENTROPIC EXPANSION OF STRANGE MATTER DROPLETS AND FORMATION OF COLD STRANGELETS

In this section we discuss the implications of the structure of the phase diagram, as it was discussed in the two preceding sections, for the expansion trajectories of hot and dense strange systems. This allows us to analyze the conditions under which the system will "get stuck" in the phase coexistence region, i.e., not hadronize completely, giving rise to surviving (meta)stable cold quark matter droplets. We will not embark here on a fully dynamical investigation of the fireball expansion, which should include, at the very least, the effects of surface evaporation (which can change the entropy and strangeness content of the system [2, 5, 6]) and the kinetics of the freeze-out

process; instead we will try to obtain first qualitative insights by assuming smooth hydrodynamic expansion at constant entropy S/A and strangeness fraction f_s.

In Figs. 6 and 7 we show isentropic expansion trajectories through the phase diagram for $B^{1/4} = 180$ and 235 MeV, respectively, for various strangeness fractions f_s. The representation differs from those in the previous sections in that we now use a two-dimensional projection of the phase diagram, with the baryon density $\rho_b(T, \mu_q, \mu_s)$ on the horizontal and the temperature on the vertical axis. In this representation, even for strangeness-neutral systems the mixed phase corresponds to a rather wide gap separating the quark and hadronic phases; this is due to the discontinuity of ρ_b in the first order phase transition. For systems with nonzero strangeness, however, the mixed phase becomes even more prominent; for the specific case of a bag constant $B^{1/4} = 180$ MeV, which is shown in Figs. 6, it extends, for a large range of temperatures below $T_c \simeq 123$ MeV and for all nonzero values of f_s, all the way to zero baryon density.

After the elaborate discussion of the zero temperature limit in Sec. III, the reason for this is clear: for $B^{1/4} = 180$ MeV, the $T = 0$ phase coexistence line runs always to the left of the thick solid line in Fig. 1 where at $T = 0$ no strange hadrons exist. Systems with finite net strangeness $f_s > 0$ therefore can reach zero temperature
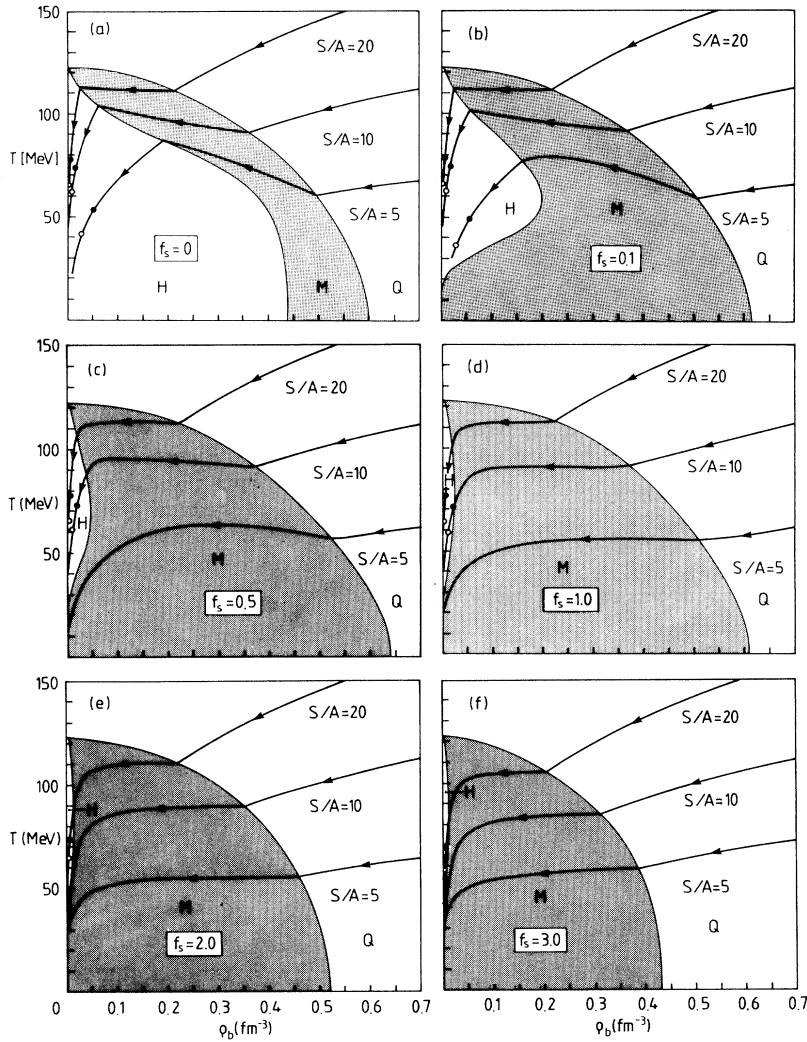
FIG. 6. Isentropic expansion trajectories and pion freeze-out in the (T, ρ_b) plane for various f_s values, for $B^{1/4} = 180$ MeV. Curves at low specific entropy S/A, which do not exit from the mixed (M) into the hadronic (H) phase, indicate strangelet formation. Pion freeze-out is indicated by full and open circles for fireball radii of 4 and 8 fm, respectively.

only by infinitely expanding to zero baryon density.

At non-zero temperature there exists a sometimes small, but finite gap of (strange) hadron gas between the T axis and the mixed phase. If the expanding quark-gluon plasma reaches this region, it hadronizes completely. The curves in Figs. 6 show that, depending on the entropy content of the system, this does not always occur: for large values of f_s and/or low values of S/A the system stays inside the mixed phase all the way to $T = 0$, $\rho_b = 0$.[3] This phenomenon sets in quite discontinuously as the system acquires finite strangeness: while for $f_s = 0$ the fireball always completes the hadronization process [see Fig. 6(a)], already at $f_s = 0.1$ all systems with $S/A \lesssim 3$ follow expansion trajectories which get trapped inside the mixed phase.

For $B^{1/4} = 235$ MeV, on the other hand, the baryon

---

[3]Since at $T = 0$ the entropy density vanishes, systems with finite specific entropy can reach zero temperature only by expanding to zero density and infinite volume.

density at the HM coexistence line is always nonzero (see Fig. 7), and an isentropically expanding fireball will therefore always hadronize completely. The formation of cold strangelets is thus impossible for such a large value of the bag constant.

Thus, within the context of isentropic, hydrodynamic expansion, the formation of cold strangelets requires a sufficiently low value for B and the expanding fireball to either possess a large strangeness fraction f_s or a low specific entropy [2]. As pointed out in Ref. [2], this is not necessarily a requirement for the initial conditions of the collision fireball, but these characteristics can, under certain conditions, be acquired dynamically, via particle radiation from the surface of the fireball in the early expansion stages. Despite the first attempts reported in [2, 5, 6], however, a convincing dynamical simulation of these phenomena does not yet exist, and we hope to return to this problem at a later point. If we assume, for example, $B^{1/4} = 180$ MeV, we see from Fig. 6 that without an efficient loss of specific entropy (i.e., entropy radiation without loss of baryon number) the fireballs from present-day heavy-ion collisions at the Brookhaven
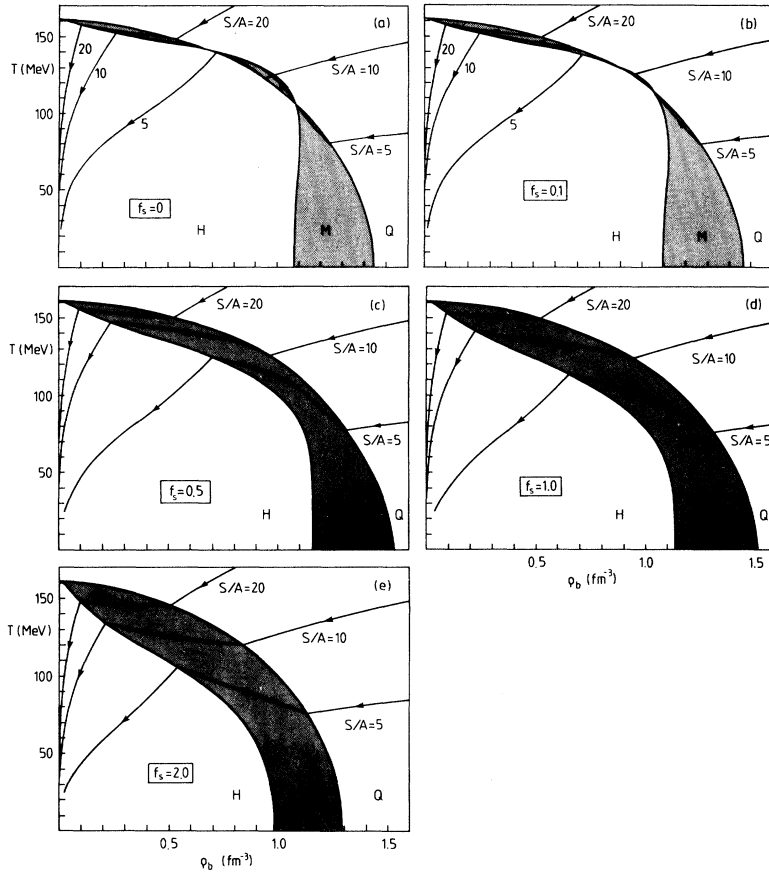
FIG. 7. Same as Fig. 6, but for $B^{1/4} = 235$ MeV. In this case all isentropic expansion trajectories exit again from the mixed phase, i.e., the fireball hadronizes completely irrespective of its specific entropy.

Alternate Gradient Synchrotron (AGS) or CERN Super Proton Synchrotron (SPS), which have been estimated to possess specific entropies in the region between $S/A = 15$ and 30 [14], would have to acquire a strangeness fraction $f_s \gtrsim 2$ to make strangelet formation possible. For smaller bag constants[4] lower values of f_s might be sufficient [2].

In Fig. 8 we summarize these findings by showing, for $B^{1/4} = 145$ and 195 MeV, respectively, the maximum specific entropy S/A compatible with the formation of cold strangelets, as a function of the strangeness fraction f_s in the fireball. While for the low value of B the window in S/A for strangelet formation is appreciable even for moderate strangeness fractions, in the case of the larger value for B the conditions on S/A are so restrictive that strangelet formation in nuclear collisions of the type presently studied appears quite unlikely. A detailed dynamical study of the fireball expansion would be needed, however, to make this statement more quantitative.

Of course, hydrodynamic expansion all the way to $T = 0$ is not a realistic assumption, since for sufficiently low temperature and density the mean free paths of the hadrons become larger than the system size, and the

hadrons decouple. The point where this happens can be estimated from the condition [15]

$$\lambda_j = R, \tag{34}$$

where

$$\lambda_j = \frac{\langle v_j \rangle_{\text{thermal}}}{\sum_i \langle \sigma_{ij} v_{ij} \rangle_{\text{thermal}} \rho_i} \tag{35}$$

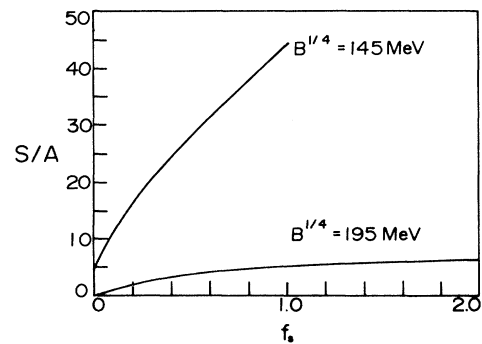is the mean free path of particle species j in a thermal

FIG. 8. The critical specific entropy for strangelet formation as a function of the strangeness fraction in the fireball, for two values of the bag constant. Only fireballs with S/A below these lines have a chance to produce surviving cold strangelets.

---

[4]Note, however, that with our equation of state $B^{1/4} \gtrsim 150$ MeV is required to ensure the stability of cold nonstrange nuclear matter against conversion into quark matter.

system, and R is the fireball radius. The sum in the denominator is over all the particle species in the fireball, weighted with their respective densities and interaction cross sections. We have evaluated Eq. (35) for pions as described in [15], and solved Eq. (34) for two fireball radii, 4 fm and 8 fm, respectively. For illustration, the corresponding freeze-out points are indicated by circles in Fig. 6.

For those trajectories in Figs. 6 which do not exit from the mixed phase, the computation of the "freeze-out point" where the hadrons outside the quark matter bubbles decouple is less straightforward. In general it requires a detailed geometrical and dynamical picture. Inclusion of the freeze-out phenomenon is, however, very important, since at this point the pressure equilibrium between the two phases is broken, and further cooling and hadronization will occur by blackbody radiation from the remaining plasma droplets [5] rather than by equilibrium phase conversion as assumed in our figures. This will be the subject of future work.

VI. SUMMARY AND CONCLUSIONS

We have presented a detailed analysis of the phase structure of cold and hot strange matter, which uncovered a rich structure in the strange sector of the quark-hadron phase diagram. Its purpose is to serve as a comprehensive and reliable thermodynamic basis for future dynamical studies of strange quark matter creation in relativistic nuclear collisions.

The thermodynamic criterion for stability of cold strange quark matter against hadronization can be phrased as $P_Q = P_H = 0$ within the region of phase coexistence; near $T = 0$ this is equivalent to $\mu_i < m_i$ for all hadronic particle species in the hadronic subphase. This condition for stability of cold strange quark matter strongly depends on the model parameters (in our case the bag constant).

Using the simple model assumptions of isentropic expansion and equilibrium hadronization, we have estimated the regions in parameter space where hot and strange quark matter could (via expansion) end up within these regions of stability, thus giving rise to strangelet formation. Thermodynamic equilibrium considerations show that strangelet formation requires relatively large

net strangeness charge combined with low specific entropy. For increasing bag constants, the window for strangelet formation closes above $B^{1/4} = 200$ MeV. Since the stability of cold, nonstrange nuclear matter against quark droplet formation requires $B^{1/4} \gtrsim 150$ MeV, the parameter range for strangelet formation is not very large. Whether the relevant regime for the thermodynamic parameters S/A and f_s can actually be reached in heavy-ion collisions must be decided on the basis of future detailed dynamical studies.

ACKNOWLEDGMENTS

APPENDIX A: EVALUATION OF THERMAL INTEGRALS IN THE LOW-TEMPERATURE LIMIT

1. Low temperature, $\mu_i > m_i$

The integrals to be evaluated in the low T limit are of the form

$$I = \int_{m_i}^{\infty} \frac{f(E)}{e^{\beta(E-\mu_i)} + 1} \, dE. \tag{A1}$$

At low temperatures, and for $\mu_i > m_i$, the Fermi distribution under the integral approximates a θ function and thus can be expanded around this limit [16]. One finds [16]

$$I = \int_{m_i}^{\mu_i} f(E) \, dE + \frac{\pi^2}{6} \frac{f'}{\beta^2} + \frac{7\pi^4}{360} \frac{f'''}{\beta^4} + \cdots, \tag{A2}$$

where the derivatives of f are taken with respect to E and evaluated at $E = \mu_i$.

For the pressure integration $f(E) = (E^2 - m_i^2)^{3/2}$, and

$$\int_{m_i}^{\infty} \frac{(E^2 - m_i^2)^{3/2}}{e^{\beta(E-\mu_i)} + 1} \, dE = \int_{m_i}^{\mu_i} (E^2 - m_i^2)^{3/2} \, dE$$
$$+ \frac{\pi^2}{2} \frac{1}{\beta^2} \mu_i (\mu_i^2 - m_i^2)^{1/2} + \frac{7\pi^4}{120} \frac{1}{\beta^4} \frac{\mu_i (2\mu_i^2 - 3m_i^2)}{(\mu_i^2 - m_i^2)^{3/2}} + \cdots. \tag{A3}$$

For the density integration $f(E) = E(E^2 - m_i^2)^{1/2}$, and

$$\int_{m_i}^{\infty} \frac{E(E^2 - m_i^2)^{1/2}}{e^{\beta(E-\mu_i)} + 1} \, dE = \int_{m_i}^{\mu_i} E(E^2 - m_i^2)^{1/2} \, dE$$
$$+ \frac{\pi^2}{6} \frac{1}{\beta^2} \frac{2\mu_i^2 - 3m_i^2}{(\mu_i^2 - m_i^2)^{1/2}} + \frac{7\pi^4}{120} \frac{1}{\beta^4} \frac{m_i^4}{(\mu_i^2 - m_i^2)^{5/2}} + \cdots. \tag{A4}$$

2. Low temperature, $\mu_i < m_i$

When $\mu_i < m_i$, we expand $1/(e^x \pm 1) = e^{-x}/(1 \pm e^{-x})$ into a power series in e^{-x} and integrate.

$$I = \int_{m_i}^{\infty} \frac{f(E)}{e^{\beta(E-\mu_i)} + 1} \, dE = \sum_{n=1}^{\infty} (\mp)^{n+1} \int_{m_i}^{\infty} f(E) \, e^{-n\beta(E-\mu_i)} \, dE. \tag{A5}$$

The pressure thus becomes

$$\frac{d_i}{6\pi^2} \int_{m_i}^{\infty} \frac{(E^2 - m_i^2)^{3/2}}{e^{\beta(E-\mu_i)} \pm 1} \, dE = \frac{d_i}{2\pi^2} \left(\frac{m_i}{\beta}\right)^2 \sum_{n=1}^{\infty} \frac{(\mp)^{n+1}}{n^2} K_2(n\beta m_i) \, e^{n\beta\mu_i} \, , \tag{A6}$$

and the density

$$\frac{d_i}{2\pi^2} \int_{m_i}^{\infty} \frac{E(E^2 - m_i^2)^{1/2}}{e^{\beta(E-\mu_i)} \pm 1} \, dE = \frac{d_i}{2\pi^2} \frac{m_i^2}{\beta} \sum_{n=1}^{\infty} \frac{(\mp)^{n+1}}{n} K_2(n\beta m_i) \, e^{n\beta\mu_i} \, , \tag{A7}$$

where $K_2(n\beta m_i)$ is the second order modified Bessel function.

In the limit $T \to 0$ ($\beta m_i \to \infty$), the asymtotic form of this Bessel function is

$$K_2(n\beta m_i) \to \sqrt{\frac{\pi}{2}} \frac{1}{\sqrt{n\beta m_i}} \, e^{-n\beta m_i} \, . \tag{A8}$$

When $\mu_i < m_i$, the above series converges rapidly in the limit $T \to 0$, and higher order terms can be neglected. Keeping only the first (Boltzmann) term with $n = 1$, we have, for $m_i > \mu_i$,

$$P_i = d_i \left(\frac{m_i}{2\pi\beta}\right)^{3/2} \frac{1}{\beta} \, e^{-\beta(m_i - \mu_i)} \, , \tag{A9}$$

$$\rho_i = d_i \left(\frac{m_i}{2\pi\beta}\right)^{3/2} e^{-\beta(m_i - \mu_i)} \, . \tag{A10}$$

3. Zero temperature

For completeness, we evaluate the Fermi integrals at $T = 0$ for $\mu_i \geq m_i$, i.e., for $x_i \equiv \mu_i/m_i \geq 1$:

$$P_i = \frac{d_i}{6\pi^2} \int_{m_i}^{\mu_i} (E^2 - m_i^2)^{3/2} \, dE$$

$$= \frac{d_i}{16\pi^2} m_i^4 \left[\ln\left(x_i + \sqrt{x_i^2 - 1}\right) - x_i\sqrt{x_i^2 - 1} + \frac{2}{3} x_i \left(x_i^2 - 1\right)^{3/2}\right] \; ; \tag{A11}$$

$$\rho_i = \frac{d_i}{2\pi^2} \int_{m_i}^{\infty} E(E^2 - m_i^2)^{1/2} \, dE$$

$$= \frac{d_i}{6\pi^2} m_i^3 \left(x_i^2 - 1\right)^{3/2} \; ; \tag{A12}$$

$$\varepsilon_i = \frac{d_i}{2\pi^2} \int_{m_i}^{\mu_i} E^2 \left(E^2 - m_i^2\right)^{1/2} \, dE$$

$$= \frac{d_i}{16\pi^2} m_i^4 \left[-\ln\left(x_i + \sqrt{x_i^2 - 1}\right) + x_i\sqrt{x_i^2 - 1} + 2x_i \left(x_i^2 - 1\right)^{3/2}\right] \; . \tag{A13}$$

At $T = 0$, bosons do not contribute to the pressure. They do contribute to the energy density if a Bose condensate exists:

$$\varepsilon_i^{\text{boson}} = m_i \, \rho_i^{\text{boson}} \, , \tag{A14}$$

where ρ_i^{boson} is the density of condensed bosons. The expressions for ε are needed for the Hagedorn proper volume correction factor.

[1] H.-C. Liu and G. L. Shaw, Phys. Rev. D **30**, 1137 (1984); **45**, 857 (1992).

[2] C. Greiner *et al.*, Phys. Rev. Lett. **58**, 1825 (1987); Phys. Rev. D **38**, 2797 (1988).

[3] E. Witten, Phys. Rev. D **30**, 272 (1984).

[4] E. Farhi and R. L. Jaffe, Phys. Rev. D **30**, 2379 (1984).

[5] H. W. Barz, B. Friman, J. Knoll, and H. Schulz, Phys. Lett. B **242**, 328 (1990).

[6] C. Greiner and H. Stöcker, Phys. Rev. D **44**, 3517 (1991).

[7] C. Dover *et al.*, "Production of rare composite objects in relativistic heavy-ion collisions," AGS Proposal No. P-864, Yale University, 1990 (unpublished); K. Pretzl *et al.*, "Search for neutral strange matter in heavy-ion collisions at CERN," SPS Proposal No. P259, CERN-SPSLC/91-16, 1991 (unpublished); C. Baglin *et al.*, "Search for strangelets and free quarks in Pb-Pb collisions," SPS Letter of Intent No. I183, CERN-SPSLC/91-41, 1991 (unpublished).

[8] C. Alcock and A. Olinto, Phys. Rev. D **39**, 1233 (1989); J. Madsen and M. Olesen, *ibid.* **43**, 1069 (1991).

[9] B. Lukács, J. Zimányi, and N. L. Balazs, Phys. Lett. B **183**, 27 (1987).

[10] U. Heinz, Kang S. Lee, and M. J. Rhoades-Brown, Mod. Phys. Lett. A **2**, 153 (1987).

[11] U. Heinz, P. R. Subramanian, H. Stöcker, and W. Greiner, J. Phys. G **12**, 1237 (1986).

[12] R. Hagedorn and J. Rafelski, in *Statistical Mechanics of Quarks and Hadrons*, edited by H. Satz (North Holland, Amsterdam, 1981), p. 237.

[13] H. W. Barz, B. Friman, J. Knoll, and H. Schulz, Phys. Rev. D **40**, 157 (1989); N. J. Davidson and H. G. Miller, Phys. Lett. B **255**, 511 (1991); J. Cleymans, J. Stålnacke, E. Suhonen, and G. M. Weber, Z. Phys. C **55**, 317 (1992).

[14] P. Lévai, B. Lukács, and J. Zimányi, J. Phys. G **16**, 1019 (1990); E. Schnedermann, Ph.D. thesis, University of Regensburg, 1992; and (unpublished); J. Letessier, A. Tounsi, and J. Rafelski, Phys. Lett. B **292**, 417 (1992).

[15] K. S. Lee and U. Heinz, Z. Phys. C **43**, 425 (1989); K. S. Lee, U. Heinz, and E. Schnedermann, Z. Phys. C **48**, 525 (1990).

[16] L. D. Landau and E. M. Lifshitz, *Statistical Physics, Part 1* (Pergamon, Oxford, 1980), Sec. 58.
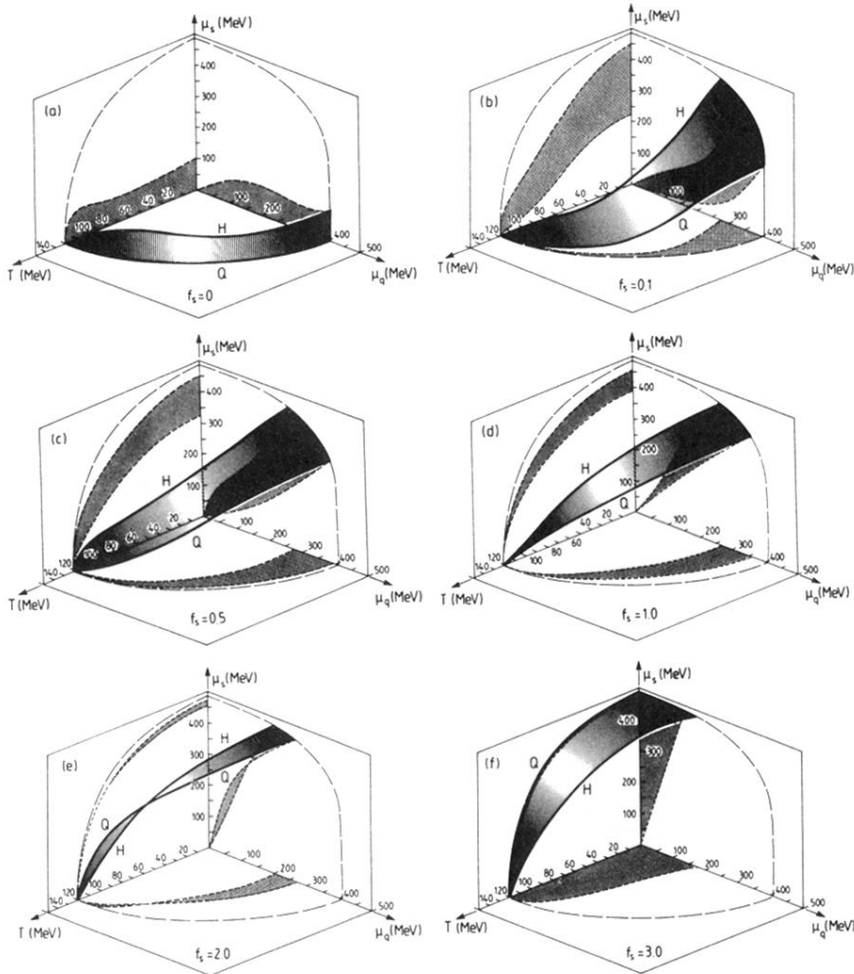
FIG. 5. The phase diagram of strongly interacting matter in (T, μ_q, μ_s) space for $B^{1/4} = 180$ MeV. The igloo-type surface describes the phase coexistence region (mixed phase) between quark matter (outside) and hadronic matter (inside). Figures (a) through (f) show various sections through this surface corresponding to systems with fixed strangeness fraction f_s. Also shown are the projections of the mixed phase region onto the three coordinate planes.
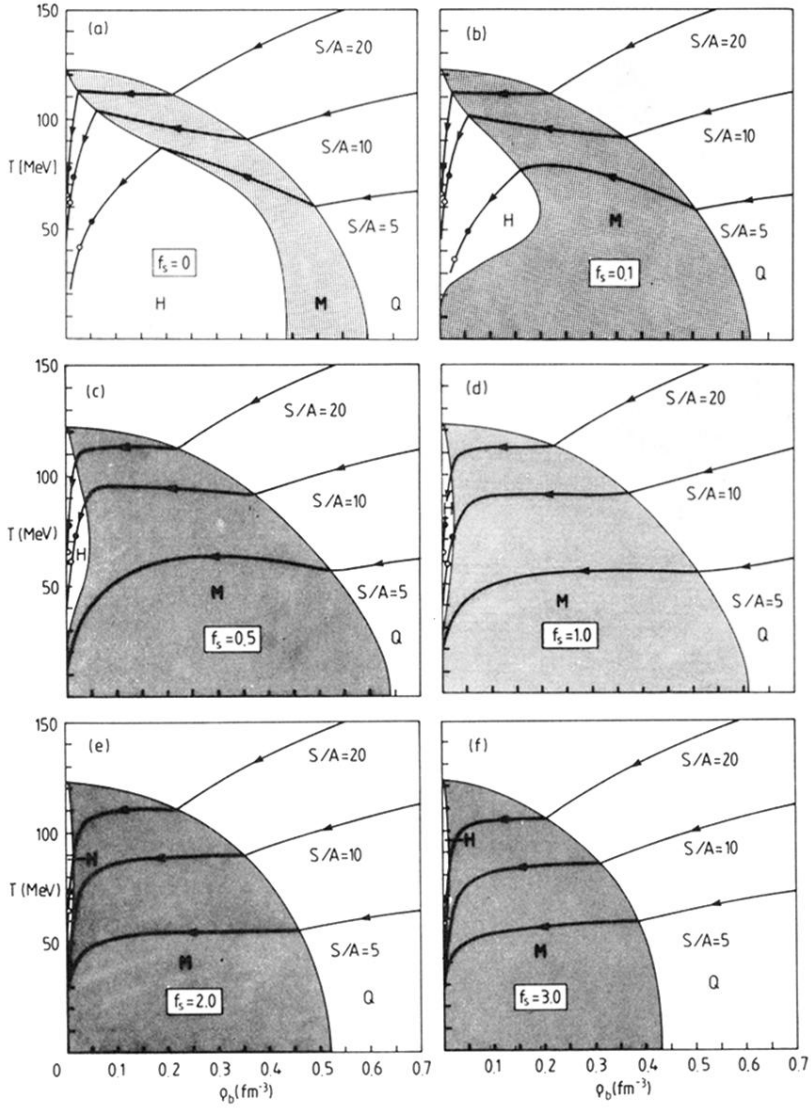
FIG. 6. Isentropic expansion trajectories and pion freeze-out in the (T, ρ_b) plane for various f_s values, for $B^{1/4} = 180$ MeV. Curves at low specific entropy S/A, which do not exit from the mixed (M) into the hadronic (H) phase, indicate strangelet formation. Pion freeze-out is indicated by full and open circles for fireball radii of 4 and 8 fm, respectively.
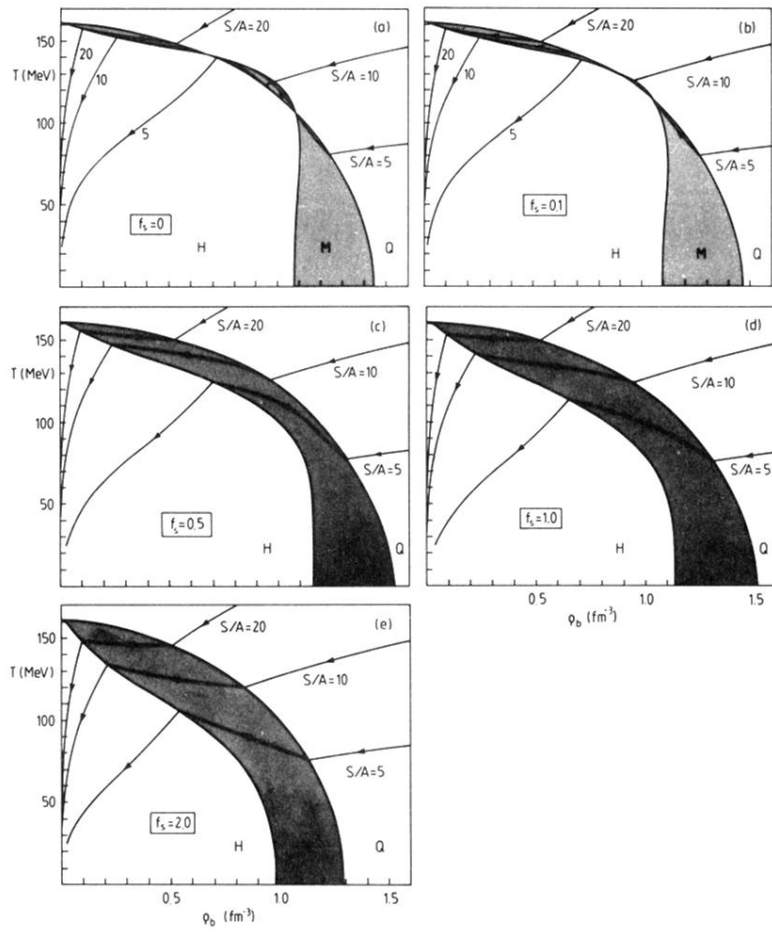
FIG. 7. Same as Fig. 6, but for $B^{1/4} = 235$ MeV. In this case all isentropic expansion trajectories exit again from the mixed phase, i.e., the fireball hadronizes completely irrespective of its specific entropy.